Received: 8 August 2017 | Accepted: 9 December 2017

DOI: 10.1002/hyp.11425

RESEARCH ARTICLE

WILEY

Seeing through porous media: An experimental study for unveiling interstitial flows

Simonetta Rubol[1,2] | Daniele Tonina[3] | Lionel Vincent[4] | Jill A. Sohm[5] | William Basham[3] | Ralph Budwig[3] | Pratixa Savalia[6] | Eva Kanso[4] | Douglas G. Capone[2] | Kenneth H. Nealson[2,6]

[1] Department of Energy Resources Engineering, Stanford University, Stanford, CA, USA

[2] Department of Biological Sciences, University of Southern California, Los Angeles, CA 90089, USA

[3] Center for Ecohydraulics Reserch, University of Idaho, 322 East Front Street, Suite 340, Boise, ID 83702, USA

[4] Department of Aerospace and Mechanical Engineering, University of Southern California, Los Angeles, CA 90089, USA

[5] Environmental Studies Program, University of Southern California, Los Angeles, CA 90089, USA

[6] Department of Earth Sciences, University of Southern California, Los Angeles, CA 90089, USA

Correspondence
Simonetta Rubol, Department of Energy Resources Engineering, Stanford University, Stanford, CA, USA.
Email: rubol@stanford.edu

Funding information
2016 Zumberge Individual Research Small Grant; National Science Foundation, Grant/Award Number: EAR1559348

Abstract

We describe a novel inexpensive method, utilizing particle image velocimetry (PIV) and refractive index-matching (RIM) for visualizing and quantifying the flow field within bio-amended porous media. To date, this technique has been limited to idealized particles, whose refractive index does not match that of fresh water and thus requires specialized and often toxic or hazardous fluids. Here, we use irregularly shaped grains made of hydrogel as the solid matrix and water as the fluid. The advantage of using water is that it provides, for the first time, the opportunity to study both hydraulic and biological processes, which typically occur in soils and streambeds. By using RIM coupled with PIV (RIM-PIV), we measured the interstitial flow field within a cell packed with granular material consisting of hydrogel grains in a size range of 1–8 mm, both in the presence and in the absence of *Sinorhizobium meliloti* bacteria (strain Rm8530). We also performed experiments with fluorescent tracer (fluorescein) and fluorescent microbes (*Shewanella GPF MR-1*) to test the capability of visualizing solute transport and microbial movements. Results showed that the RIM-PIV can measure the flow field for both biofilm-free and biofilm-covered hydrogel grains. The fluorescent tracer injection showed the ability to visualize both physical (concave surfaces and eddies) and biological (biofilms) transient storage zones, whereas the fluorescent microbe treatment showed the ability to track microbial movements within fluids. We conclude that the proposed methodology is a promising tool to visualize and quantify biofilm attachment, growth, and detachment in a system closer to natural conditions than a 2D flow cell experiment.

KEYWORDS

biofilm, hydrogel, irregular granular particles, particle image velocimetry (PIV), porous media flow, refractive index-matching (RIM)

1 | INTRODUCTION

Flow within porous media is important in many engineering, medical, and biological applications (Häfeli, Altheimer, Butscher, & von Rohr, 2014; Patil & Liburdy, 2013) given its pivotal role in regulating the stability and performance of reaction rates (Boisson, Roubinet, Aquilina, Bour, & Davy, 2014). A powerful nonintrusive method to measure the flow field around solid objects is particle image velocimetry (PIV), which allows for visualization of the flow field within solid objects such as pipes and granular materials when coupled with refractive index-matching (RIM; Adrian & Westerweel, 2011). In RIM-PIV, both fluid and solid objects have the same refractive index, preventing distortion and blockage of the laser light sheet used in PIV (Budwig, 1994). Previous studies of porous media flow with the RIM-PIV method have been limited to granular material consisting of glass spheres of the same diameter or irregular silica grains (Häfeli et al., 2014; Wood et al., 2015) that refractively match toxic or hazardous fluids (e.g., mineral oil). This has prevented the visualization and quantification of the flow field in granular porous media made with grains of different diameters and shapes (e.g., Holzner, Morales, Willmann, & Dentz, 2015; Sidler, Michalec, Detert, & Holster, 2016), as well as the analyses of microbial colonization of complex three-dimensional surfaces such as those typically found in soils and sediments. A few previous studies used the

transparent solid Nafion, which has a refractive index (RI) of 1.37 (or RI = 1.35 reported by Leis, Schlicher, Franke, & Strathmann, 2005), to visualize the growth and formation of biofilms (Drescher, Shen, Bassler, & Stone, 2013; Leis et al., 2005) and root systems (Downe et al., 2012) in porous media. However, they could not apply RIM-PIV with fresh water because of the prohibitive differences of their refractive indexes (Nafion RI = 1.35 and fresh water RI = 1.333). Hydrogel has a RI that matches that of fresh water, but studies on the use of the RIM-PIV method with hydrogel have so far been limited to the visualization of flow within a staggered array of cylinders (Weitzman, Samuel, Craig, Zeller, & Monismith, 2014 and references herein cited) and the interaction of red blood cells (Rahgozar, Rosi, Kaucky, Walker, & Rival, 2015).

Here, we use hydrogel to mimic soil and sediment grains and investigate for the first time whether the RIM-PIV method works as the grains get progressively covered with biofilm, especially with extracellular polymeric substances (EPS), a self-produced matrix in which microbes are embedded (Romaní et al., 2008; Rosenzweig, Shavit, & Furman, 2012). The suitability of hydrogel as a proxy for soil particles has been analysed elsewhere (e.g., Tabe, 2015). Briefly, a hydrogel packed bed resembles the hydraulic conductivity of natural soils in the range of 10^{-2} to 10^{-8} cm/s and exhibits macro-scale geotechnical properties similar to the ones of natural soil especially sandy and silty soil (see Table 3 of Tabe, 2015 and Table 1 of Iskander, Bathurst, & Omidvar, 2015). It has a compression index of 0.1–0.15 and a recompression index of 0.002–0.005, and it is suitable to model flow of water in soils and marine deposits. We refer to Iskander et al. (2015) and Tabe (2015) for a thorough review on the topic.

We formed hydrogel into irregular particles with diameters ranging between 1 and 8 mm. These grains mimic the size of pea gravel material, but they can be made as coarse or fine as needed. We created a packed bed of the particles to demonstrate that RIM-PIV can be used to measure the interstitial flow velocities at micron scale under different treatment conditions: (a) with fresh water; (b) with media for microbial growth; and (c) with microbial community attachment, growth, and formation of biofilm and EPS. We were also able to visualize (d) transient storages of solutes (fluorescein dye) in the pores and (e) a moving plume of fluorescent microbes.

2 | METHODS

For our experiment, we used a 10 cm height cell with a square cross section of 5 by 5 cm. All components were autoclaved and washed with 10% peroxyacetic acid. The pieces were then assembled in a biologically safe cabinet to prevent contamination. Fluid entered the cell from the bottom through a tube connected to a Marriott-type water tank (whose air intake had a filter to prevent any external contamination) and exited from the top through a tube emptying into a small holding tank for later analysis of the outlet water (Figure 1).

The flow cell was packed with hydrogel grains (Figures 1 and 2a). We followed the procedure of Weitzman et al. (2014) and Menter (2016) to create hydrogel slabs from sodium polyacrylate-co-polyacrylamide hydrogel and deionized water. The resulting hydrogel slabs had a 99.02% water content by mass (and 0.98% of polymer) and a RI of 1.3327. We then pressed them through sieves with 8 and 2 mm openings. This operation fractured the hydrogel into grains of irregular shape with sizes ranging between approximately 1 and 8 mm. The grain size distribution had a median grain size of 4.76 mm and a standard deviation of 0.52 mm (the granulometric curve is included in Figure S1).

We used PIV with micron resolution to investigate the fluid motion around the hydrogel particles in a cross section of the cell illuminated by a vertical laser sheet. The cross section was selected such that there was 1 cm of medium and grains between the PIV plane and the camera lens. The entering water was seeded with 4-µm bio-compatible sulfate microspheres. These fluorescent particles are small enough and almost neutrally buoyant (density of 1.055 g/cm^3), making them suitable flow tracers. Their downward settling velocity is approximately 0.5 µm/s, much smaller than the typical velocities found in the flow cell (10–100 µm/s). Images were recorded using a Point Grey Grasshopper 3 high-resolution (2048 × 2048px, 4 MPix) camera and processed with the open-source MATLAB app PIVlab (Thielicke &

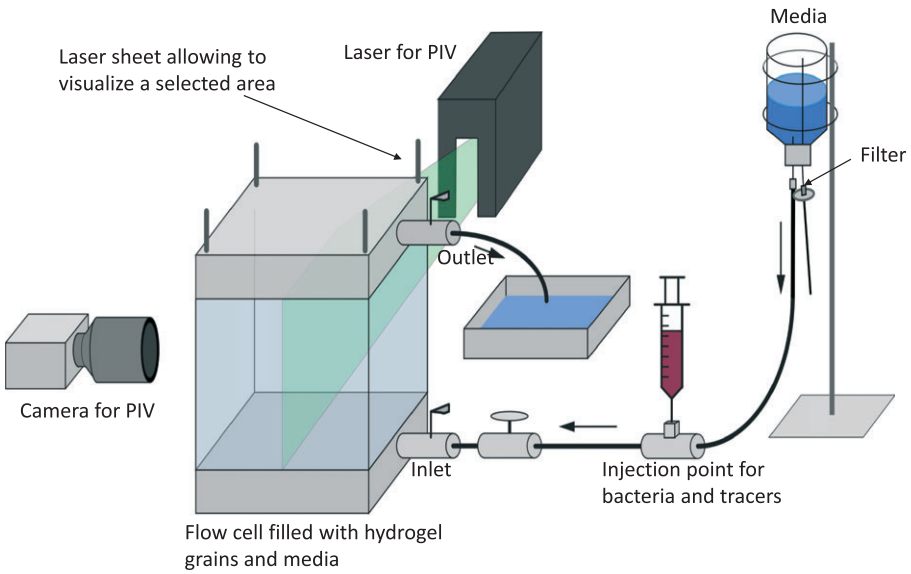

FIGURE 1 Experimental set-up. PIV = particle image velocimetry

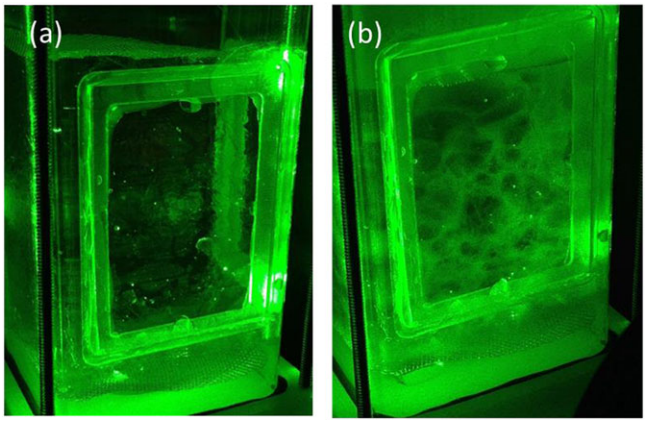

FIGURE 2 (a) The flow cell filled with hydrogel and media (M9) or deionized water (M9), (b) the flow cell after the addition of *Sinorhizobium meliloti*

Stamhuis, 2014), which uses a fast Fourier transform-based algorithm with multipass and window deformation. Typical window size was 32 px (enclosing at least 15 particles), with 50% overlap between adjacent windows. Preprocessing steps involved defining the region of interest and masking the areas where no flow is present (hydrogel grains). The only post-processing step was to discard spurious vectors based on their magnitude. To this aim, we plotted the horizontal and vertical magnitudes of the vectors of the whole PIV sequence in a single plot. We then discarded those vectors whose horizontal or vertical magnitude exceeded a specified threshold (the threshold was set by hand, based on at least 50 vector fields from the same sequence). This step discarded about 2–5% of all vectors. The shutter time was set to 10 ms, ensuring that particles were not motion blurred. The time interval was adjusted between 0.2 and 2 s so that the maximum particle displacement between two successive frames was about 5 pixels, and the average was around 1 pixel, minimizing both noise and correlation error (Raffel, Willert, Wereley, & Kompenhans, 1998). Moreover, the field of view was adjusted so that the apparent particle size was around 1 pixel, ensuring the largest field of view with minimal deterioration of measurement performance (Westerweel, 2000).

We determined the baseline velocity field in the porous media for a water inflow of 0.05 cm^3/min. Then, we grew biofilm in the cell; *Sinorhizobium meliloti*, strain Rm8530, was chosen because of its mucoid characteristic, which is due to the overproduction of EPSs. *S. meliloti* culture was prepared for injection into the flow cell by growing it overnight in Tryptone Yeast broth. The culture was centrifuged twice at 4,226 × *g* for 5 min. Pelleted cells were suspended in M9 minimal media with 0.4% glycerol following the procedure described in Deng et al. (2015). Microbial addition for biofilm growth was performed using an 80 ml sterilized syringe containing 2.5×10^4 *S. meliloti* cells. The flow was stopped for 2 hr right after the injection to promote the attachment of the bacteria on the hydrogel grains. Then, the flow was started again and growth of the biofilm occurred over 5 days.

After 10 days, we performed a tracer test with fluorescein to observe whether the biofilms can absorb the injected fluid and thus whether microbe-produced substances work as a transient storage of solutes (Or, Phutane, & Dechesne, 2007; Rubol et al., 2014). The tracer test with fluorescein was performed by injecting the tracer from the bottom of the flow cell and stopping the flow for 15 hr. Next, the flow was restored (without fluorescein injection), and pictures were collected after the excess of fluorescein in the pore space was washed out, to look at the trapped pockets of fluorescein within the EPS and the dead zones of the porous media.

The capability of the system to track bacteria was tested with *Shewanella* GFP MR-1, a fluorescent microbe with versatile accepting capacities (Fredrickson et al., 2008). *Shewanella* GFP MR-1 was grown in batch culture using Luria-Bertani medium with 50 μg/ml Kanamycin to an optical density of 2 to 2.5 when measured at 600 nm wavelength. The culture was centrifuged twice at 4,226 × *g* for 5 min. Pelleted cells were suspended in defined medium containing 25 mM PIPES [piperazine-*N*,*N*_-bis(2-ethanesulfonic acid)], 24 mM NaHCO3, 7.5 mM NaOH, 28 mM NH4Cl, 1.3 mM KCl, 4.3 mM NaH2PO4-H2O, and 10 ml/L of vitamins, amino acids, and trace minerals (Pirbadian et al., 2014). The pH was adjusted to 7.2. Lactate (20 mM) was added as the carbon source and the culture was grown aerobically as described by Pirbadian et al. (2014). *Shewanella* cells were then stained with FM® 4-64FX (ThermoFisher), which has an emission wavelength close to that of the laser (532 μm), such that microbes would be visible within the laser light sheet used for PIV. This suspension of *Shewanella* GFP MR-1 cells was injected in the bio-amended porous media using a 5 ml sterile syringe.

Confocal microscopy and scanning electron microscopy (SEM) analyses were used postexperiment to corroborate the presence of biofilms. Confocal laser scanning microscope analyses were performed at the Translational Imaging Center at USC. Samples were stained with SYBR® Green (ThermoFisher) for DNA and Concanavalin A, Alexa Fluor® 633 Conjugate (TermoFisher) for EPS. SEM analysis was performed at CEMMA, USC's Center for Electron Microscopy and Micro-Analysis. Samples were fixed in 2.5% glutaraldehyde and dehydrated with an increasing ethanol concentration series ranging from 30% to 100%. Samples were then dried using a critical point dryer (Tousimis) and sputter coated (Cressington) using a Pd/Pt alloy target.

3 | RESULTS

The pulse injection of *S. meliloti* Rm8530 to the system temporarily filled the pores with bacteria, which attached to the surface of the hydrogel grains and promoted biofilm formation with a large production of EPS (Figure 2b and Figure S2). Biological analysis of the outflow water showed an increasing number of *S. meliloti* cells with time, indicating that they were growing and reproducing in the system. EPS, visible to the naked eye as white slimy inclusions, appeared 5 days after *S. meliloti* injection and became highly visible within 9 days (Figure S2) both in the pore space and attached to the hydrogel (c.f. Figure 2a,b). The confocal image (Figure 3a) and SEM (Figure 3b) analyses confirmed the presence of microbes and EPS attached to the surface of the hydrogel grains.

The presence of the biofilm did not affect the uniformity of the laser sheet illumination. PIV images were recorded at different stages of the biofilm formation without any loss of resolution showing that RIM-PIV performed well for all cases: (a) hydrogel and water, (b) hydrogel and media, and (c) hydrogel colonized by microbes (Figures 2 and 4). This shows that laser acquisition is possible in the presence of

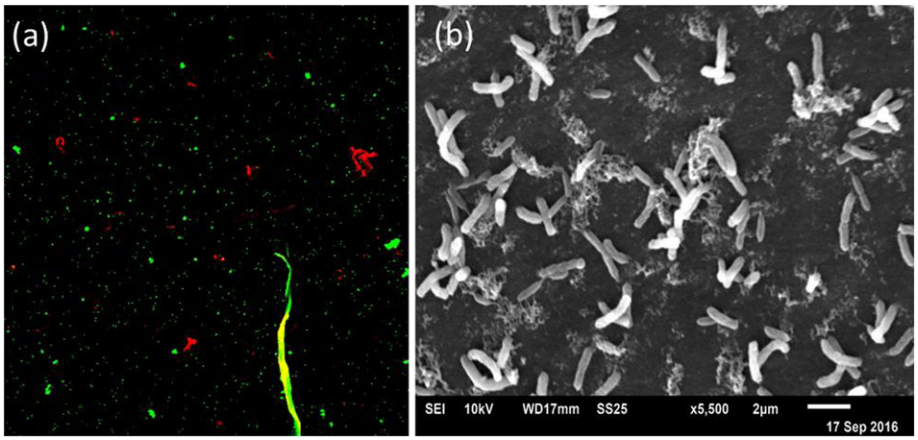

FIGURE 3 (a) Microbial (in green) and extracellular polymeric substance (in red) attachment on hydrogel surface using confocal imaging (field view 1.2 × 1.2 mm) and (b) scanning electron microscopy

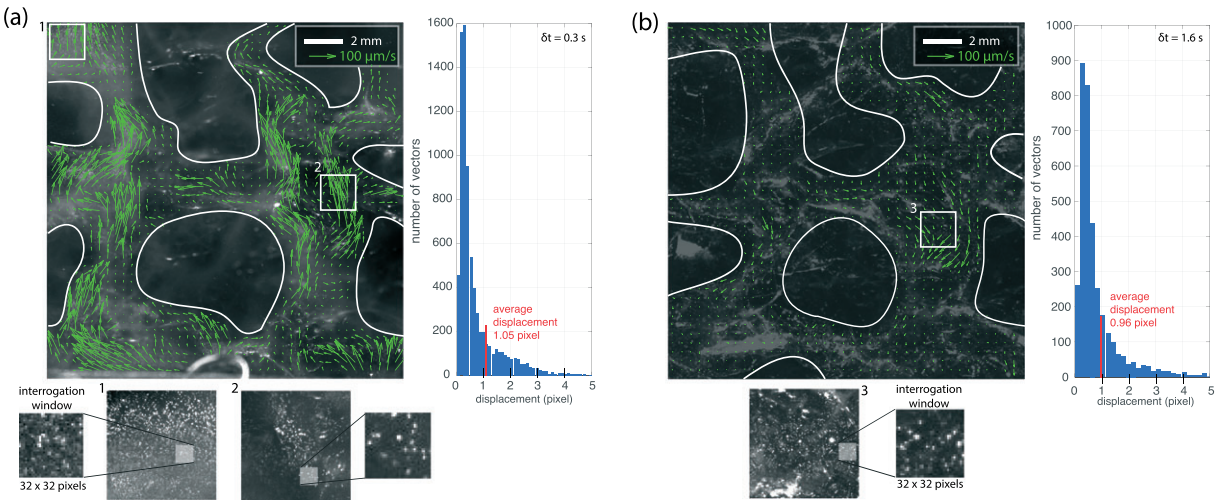

FIGURE 4 Flow-field measured (a) before biofilm formation and (b) after biofilm formation, when the flow cell was filled with hydrogel and media (M9). Inlets and histograms indicate the excellent quality of the particle image velocimetry for amended and unamended porous media

highly mucoid bacteria, such as *S. meliloti*. The small flow velocities enabled the use of high-resolution cameras at their maximum resolution and lowest gain/ISO setting, ensuring the highest signal/noise ratio. The image quality itself was remarkably good, even though there was 1 cm of medium and grains between the PIV plane and the camera lens. Figure 4 includes insets that demonstrate the image quality in three different corners. Overall, crisp and noise-free images generated favourable conditions for PIV. The number of spurious (aberrant) vectors for each processed frame was less than 2% from the post-processing analysis. Also, as shown by the left panel of Figure 4a,b, the distribution of displacement vectors was smooth: No peak locking was observed in either case.

It should be noted that time-averaging could be applied to the PIV measurements to improve the signal-to-noise ratio because the flow is steady, as would be expected from the low Reynolds number (Re) characterizing the flow in the pores: Re < 0.2. The Videos S1 and S2 demonstrate that the flow field is independent of time. However, we emphasize that the flow fields shown in Figure 4 are not time-averaged but instantaneous. Although the present PIV measurements and videos (S1 and S2) did not quantify the velocity component normal to the laser illumination plane, they do indicate the presence of a highly complex three-dimensional flow field due to the irregular hydrogel grains (Figure 4a) with dead zones, tortuous paths, contractions, expansions, and vortices. An example of the flow field measured in the bio-amended hydrogel is shown in Figure 4b, where the "white material" in the background image corresponds to fluorescent particles trapped in the dead zones and on/within the EPS. Both images have the same field of view and overall flow rate through the cell. However, the flow field is quite different due to two reasons: (a) the bio-clogging of the pores from biofilm growth and (b) a 30% shrinking of the hydrogel grains. Shrinking of the hydrogel grains was observed after the fluid was changed from water to media for the biofilm growth.

The presence of seeding particles either embedded in the EPS or in the dead zones was highlighted by the fluorescein test, indicating that EPS can act as a bio-storage of solutes (Figure 5). Further analysis of hydrogel and minimal media collected from the flow cell revealed the presence of *S. melitoti* and EPS attached on the hydrogel surface and also present in the interstitial media.

In contrast to fluorescent particles, the camera was not able to track single cells of GFP MR-1 *Shewanella*, even when stained with

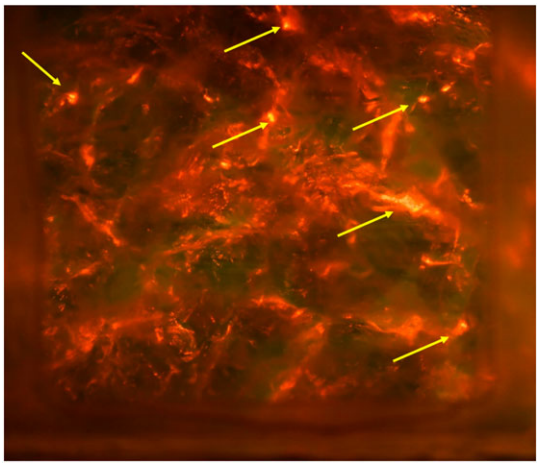

FIGURE 5 Bio-storage of solutes and particles into the extracellular polymeric substances (EPS) produced by the *Sinorhizobium meliloti* cells. Note the fluorescein and particles absorbed by the EPS structure after the drainage of the flow cell. This indicates the capability of microbe-produced substances to storage solutes. Arrows point to areas where fluorescein was highly accumulated, which correspond to EPS and/or dead zones

FM® 4-64FX. Given that the resolution of the camera is effectively 4 μm per pixel, whereas *Shewanella* cells are 1–2 μm in length, we were not able to identify FM® 4-64FX stained *Shewanella* within the interstices after the injection. However, were able to detect a plume of stained *Shewanella* at the top of the flow cell (Figure S3 and Video S3).

4 | DISCUSSION

This work shows that RIM-PIV can be used to measure the interstitial flow velocities at micron scale with (a) fresh water; (b) media for microbial growth; and (c) bacteria and EPS covering the grains in packed beds. Whereas previous works used regular spherical beads and biofilm-free porous media, our work focused on the use of PIV with irregular grains colonized by biofilm. The transparent soil made by hydrogel grains with irregular shape mimics sand and pebble size grains (Tabe, 2015; Iskander et al., 2015) and thus provides the opportunity to investigate complex three-dimensional flows within porous media and the formation, colonization, and evolution of microbial communities within sediments. Our results show that microbes attached and developed EPS, and their presence did not affect PIV measurements.

The ability to have irregular shapes similar to natural grains is paramount for the study of hydrological, mixing, and biological processes, because of the role of pockets, concavities, and convexities present on the grain surface in storing, sheltering, and mixing solutes and microbes. These irregularities create large contact surfaces that affect the formation of recirculating zones, and the growth, shape, and thickness of biofilms. In addition, the ability to make irregular porous media is promising for the study of biofilm formation in human tissues (Khaled & Vafai, 2003).

We point out that hydrogel grains will expand and contract when exposed to media with distinct solute concentration (i.e., other than the one used to make the hydrogel). The hydrogel was made and stored with deionized water. However, the media flowing through the cell was rich in nutrients. This created an osmotic difference between the grains and the fluid that modified the volume of the hydrogel grains resulting in a 30% contraction of the grain size, which then stabilized and remained constant. This issue can be solved by soaking the hydrogel grains in the media until stabilized (typically 1 day) and then used in the experiment.

Our preliminary tests showed that the limitation of using GFP MR-1 *Shewanella* as seeding particles was the camera resolution. A higher resolution camera or higher optical magnification system would have been able to distinguish individual microbes. Despite, we were able to detect the plume of MR-1 *Shewanella* stained with FM® 4-64FX (Figure S3) with the current set-up. The use of FM® 4-64FX seems promising, because it has an emission wavelength close to the one of the laser (532 μm). Using *Shewanella* as seeding particles will allow the study of biofilm attachment and the capability of EPS to store bacterial pathogens and viruses. In the latter, *Shewanella* will act as a proxy for bacterial pathogens. We are currently applying this methodology to study the effect of wetting and drying on biofilm formation and on the viability of pathogens. In addition, results indicate that hydrogel grains are suitable to be analysed via confocal microscopy, although the irregular shape of the grains may hamper the visualization of a large portion of the hydrogel surface. SEM showed bacteria dotting the hydrogel surface, however, the sample preparation process may alter the amount of microbes present on the surface.

The method we propose is by far simpler and less expensive than other existing experimental techniques, such as magnetic resonance imaging or microtomography. Extension to full three-dimensional components of the velocity field can be promptly obtained by using stereo-PIV. In the future, we will expand this method to include (a) a natural community of bacteria instead of a single strain, (b) seawater to create the hydrogel pellet for the study of marine sediments, and (c) fluorescent bacteria strains as seeding particles. Once the above aspects are implemented, our methodology can potentially be applied to different research areas such as (a) bioremediation of contaminated sites, (b) biofilm formation in natural freshwater and marine environments, and (c) bio-clogging including 3D changes in the flow, the probability density function (pdf) of velocity, and volume of biofilms as biofilm develops. We conclude that the proposed methodology is a promising tool to visualize and quantify biofilm attachment, growth, and detachment in a system closer to natural conditions than a 2D flow cell experiment.

ACKNOWLEDGMENTS

This research was partially funded by the National Science Foundation award number EAR1559348 and the 2016 Zumberge Individual Research Small Grant. We thank Dan Gage and Reed Goodwin for providing us the *S. meliloti* strain and Sahand Pirbadian for helping with the FM® 4-64FX stain. Any opinions, conclusions, or recommendations expressed in this letter are those of the authors and do not necessarily reflect the views of the supporting agency.

ORCID

Simonetta Rubol http://orcid.org/0000-0002-2418-9309
Daniele Tonina http://orcid.org/0000-0002-1866-1013

REFERENCES

Adrian, R. J., & Westerweel, J. (2011). *Particle image velocimetry*. Cambridge: New York.

Boisson, A., Roubinet, D., Aquilina, L., Bour, O., & Davy, P. (2014). Impact of flow velocity on biochemical processes—A laboratory experiment. *Hydrology and Earth System Sciences Discussions*, *11*(8), 9829–9862.

Budwig, R. (1994). Refractive index matching methods for liquid flow investigations. *Experiments in Fluids*, *17*, 350–355.

Deng, J., Orner, E. P., Chau, J. F., Anderson, E. M., Kadilak, A. L., Rubinstein, R. L., & Shor, L. M. (2015). Synergistic effects of soil microstructure and bacterial EPS on drying rate in emulated soil micromodels. *Soil Biology and Biochemistry*, *83*, 116–124.

Downe, H., Holden, N., Otten, W., Spiers, A. J., Valentine, T. A., & Dupuy, L. X. (2012). Transparent soil for imaging the rhizosphere. *PLoS One*, *7*(9), e44276. https://doi.org/10.1371/journal.pone.0044276

Drescher, K., Shen, Y., Bassler, B., & Stone, H. A. (2013). Biofilm streamers cause catastrophic disruption of flow with consequences for environmental and medical systems. *Proceedings of the National Academy of Sciences of the United States of America*, *110*(11), 4345–4350. https://doi.org/10.1073/pnas.1300321110

Fredrickson, J. K., Romine, M. F., Beliaev, A. S., Auchtung, J. M., Driscoll, M. E., Gardner, T. S., … Rodionov, D. A. (2008). Towards environmental systems biology of Shewanella. *Nature Reviews Microbiology*, *6*(8), 592–603.

Häfeli, R., Altheimer, M., Butscher, D., & von Rohr, R. P. (2014). PIV study of flow through porous structure using refractive index matching. *Experiments in Fluids*, *55*. https://doi.org/10.1007/s00348-014-1717-5

Holzner, M., Morales, V. L., Willmann, M., & Dentz, M. (2015). Intermittent lagrangian velocities and accelerations in three-dimensional porous medium flow. *Physical Review E*, *92*(1), 013015.

Iskander, M., Bathurst, R. J., & Omidvar, M. (2015). Past, present and future of transparent soils. *Geotechnical Testing Journal*, *38*(5), 557–573. https://doi.org/10.1520/GTJ20150079

Khaled, A.-R. A., & Vafai, K. (2003). The role of porous media in modeling flow and heat transfer in biological tissues. *International Journal of Heat and Mass Transfer*, *46*(26), 4989–5003.

Leis, A. P., Schlicher, S., Franke, H., & Strathmann, M. (2005). Optically transparent porous medium for nondestructive studies of microbial biofilm architecture and transport dynamics. *Applied and Environmental Microbiology*, *71*(8), 4801–4808. https://doi.org/10.1128/AEM.71.8.4801%E2%80%934808.2005

Menter, P. (2016), Tech note 1156: Acrylimide polymerization—A practical approach, edited, Bio-rad laboratories, Hercules, CA.

Or, D., Phutane, S., & Dechesne, A. (2007). Extracellular polymeric substances affecting pore-scale hydrologic conditions for bacterial activity in unsaturated soils. *Vadose Zone Journal*, *6*(2), 298–305. https://doi.org/10.2136/vzj2006.0080

Patil, V. A., & Liburdy, J. A. (2013). Flow characterization using PIV measurements in a low aspect ratio randomly packed porous bed. *Experiments in Fluids*, *54*. https://doi.org/10.1007/s00348-013-1497-3

Pirbadian, S., Barchinger, S. E., Leung, K. M., Byun, H. S., Jangir, Y., Bouhenni, R. A., … Gorby, Y. A. (2014). Shewanella oneidensis MR-1 nanowires are outer membrane and periplasmic extensions of the extracellular electron transport components. *Proceedings of the National Academy of Sciences*, *111*(35), 12883–12888.

Raffel, M., Willert, C. E., Wereley, S. T., & Kompenhans, J. (1998). *Particle image velocimetry: A practical guide*. Berlin: Springer. https://doi.org/10.1007/978%C2%AD3%C2%AD662%C2%AD03637%C2%AD2

Rahgozar, S., Rosi G. A., Kaucky L., Walker A., & Rival D. E. (2015), Exploring the interaction of red blood cell analogs with turbulence using particle tracking velocimetry, international symposium on turbulence and shear flow phenomena, 30 June 2015, melburne, Australia.

Romaní, A. M., Fund, K., Artigas, J., Schwartz, T., Sabater, S., & Obst, U. (2008). Relevance of polymeric matrix enzymes during biofilm formation. *Microbial Ecology*, *56*, 427–436.

Rosenzweig, R., Shavit, U., & Furman, A. (2012). Water retention curves of biofilm-affected soils using xanthan as an analogue. *Soil Science Society of America Journal*, *76*(1), 61–69. https://doi.org/10.2136/sssaj2011.0155

Rubol, S., Freixa, A., Carles-Brangarí, A., Fernàndez-Garcia, D., Romaní, A. M., & Sanchez-Vila, X. (2014). Connecting bacterial colonization to physical and biochemical changes in a sand box infiltration experiment. *Journal of Hydroglogy*, *517*, 317–327. https://doi.org/10.1016/j.jhydrol.2014.05.041

Sidler, D., Michalec, F. G., Detert, M., & Holster, M. (2016). Three-dimensional tracking of the motion of benthic copepods in the free water and inside the transparent sediment bed of a laboratory flume. *Limnology and Oceanography. Methods*.

Tabe, Kazunori. (2015), "Transparent Aquabeads to model LNAPL ganglia migration through surfactant flushing." 787-804.

Thielicke, W., & Stamhuis, E. J. (2014). Pivlab—Towards user-friendly, affordable and accurate digital particle image velocimetry in matlab. *Journal of Open Research Software*, *2*(1).

Weitzman, J. S., Samuel, L. C., Craig, A. E., Zeller, R. B., & Monismith, J. R. (2014). On the use of refractive-index-matched hydrogel for fluid velocity measurement within and around geometrically complex solid obstructions. *Experiments in Fluids*, *55*(12). https://doi.org/10.1007/s00348-014-1862-x

Westerweel, J. (2000). Effect of sensor geometry on the performance of PIV interrogation. In *Laser techniques applied to fluid mechanics* (pp. 37–55). Berlin: Springer.

Wood, B. D., Apte, S. V., Luburdy, J. A., Ziazi, R. M., He, X., Finn, J. R., & Patil, V. A. (2015). A comparison of measured and modeled velocity fields for a laminar flow in a porous medium. *Advances in Water Resources*, *85*, 45–63.

SUPPORTING INFORMATION

Additional Supporting Information may be found online in the supporting information tab for this article.

How to cite this article: Rubol S, Tonina D, Vincent L, et al. Seeing through porous media: An experimental study for unveiling interstitial flows. *Hydrological Processes*. 2018;32: 402–407. https://doi.org/10.1002/hyp.11425